Brief Communications

Temporal Integration of Cholinergic and GABAergic Inputs in Isolated Insect Mushroom Body Neurons Exposes Pairing-Specific Signal Processing

Davide Raccuglia and Uli Mueller

Department 8.3 Biosciences, Zoology/Physiology-Neurobiology, ZHMB (Center of Human and Molecular Biology), Natural Science and Technology III, Saarland University, D-66041 Saarbrücken, Germany

GABAergic modulation of neuronal activity plays a crucial role in physiological processes including learning and memory in both insects and mammals. During olfactory learning in honeybees (*Apis mellifera*) and *Drosophila melanogaster* the temporal relation between excitatory cholinergic and inhibitory GABAergic inputs critically affects learning. However, the cellular mechanisms of temporal integration of these antagonistic inputs are unknown. To address this question, we use calcium imaging of isolated honeybee and *Drosophila* Kenyon cells (KCs), which are targets of cholinergic and GABAergic inputs during olfactory learning. In the whole population of honeybee KCs we find that pairing of acetylcholine (ACh) and γ-aminobutyric acid (GABA) reduces the ACh-induced calcium influx, and depending on their temporal sequence, induces different forms of neuronal plasticity. After ACh–GABA pairing the calcium influx of a subsequent excitatory stimulus is increased, while GABA–ACh pairing affects the decay time leading to elevated calcium levels during the late phase of a subsequent excitatory stimulus. In an exactly defined subset of *Drosophila* KCs implicated in learning we find similar pairing-specific differences. Specifically the GABA–ACh pairing splits the KCs in two functional subgroups: one is only weakly inhibited by GABA and shows no neuronal plasticity and the other subgroup is strongly inhibited by GABA and shows elevated calcium levels during the late phase of a subsequent excitatory stimulus. Our findings provide evidence that insect KCs are capable of contributing to temporal processing of cholinergic and GABAergic inputs, which provides a neuronal mechanism of the differential temporal role of GABAergic inhibition during learning.

Key words: **ACh; calcium; GABA; Kenyon cell; mushroom body**

Introduction

The balance and temporal relation between the inhibitory neurotransmitter GABA and excitatory neurotransmitters like ACh and glutamate are of central importance for the regulation of numerous physiological processes including neuronal plasticity in memory networks (Vogels et al., 2011). Imbalances in mice can be induced by knock-out of specific $GABA_A$ receptors and demonstrate that GABAergic inhibition is critically involved in learning and memory (DeLorey et al., 1998; Collinson et al., 2002). In *Drosophila* GABAergic inhibition of the Kenyon cells (KCs) of the mushroom bodies (MBs), a brain structure essential for learning (de Belle and Heisenberg, 1994), modulates memory acquisition: elevated expression of $GABA_A$ receptor subunits in the KCs diminishes olfactory learning, whereas knockdown facilitates learning (Liu et al., 2007; Liu and Davis, 2009). While these studies show that GABAergic inhibition impairs learning, other studies suggest that GABAergic inhibition after learning is necessary for the formation of short-term memory (Pitman et al., 2011). We recently made a similar finding during associative learning in the honeybee demonstrating that the temporal relation between excitatory and inhibitory stimuli is of central importance for processes of memory formation (Raccuglia and Mueller, 2013). We used uncaging of GABA and found that GABAergic inhibition only affected processes of memory formation before and during associative pairing but not instantly afterward. Electrophysiological and optical recordings during olfactory associative learning also indicate a temporal role for cholinergic and GABAergic input into KCs: during olfactory stimulation (conditioning stimulus, CS) KCs receive cholinergic input from projection neurons and GABAergic feedback inhibition (anterior paired lateral neurons in *Drosophila* and GABAergic feedback neurons in honeybees; Gronenberg, 1987; Grünewald, 1999; Liu and Davis, 2009; Lin et al., 2014). During reward or punishment (unconditioned stimulus, US) the same GABAergic neurons are activated by sugar in honeybees (Grünewald, 1999) and by electric shock in *Drosophila* (Liu and Davis, 2009) without activating cholinergic projection neurons. Thus it is very likely that during olfactory conditioning (CS–US pairing) the temporal relation of

Received Feb. 18, 2014; revised Sept. 20, 2014; accepted Oct. 21, 2014.

Author contributions: D.R. and U.M. designed research; D.R. performed research; U.M. contributed unpublished reagents/analytic tools; D.R. and U.M. analyzed data; D.R. and U.M. wrote the paper.

We thank A. Gardezi for technical support and Dr. S. Meuser for help with this manuscript.

The authors declare no competing financial interests.

D. Raccuglia's present address: Department of Cellular and Molecular Physiology, Yale School of Medicine, New Haven, Connecticut 06510.

Correspondence should be addressed to Uli Mueller, Department 8.3 Biosciences, Zoology/Physiology (Neurobiology), Natural Science and Technology III, Saarland University, D-66041 Saarbrücken, Germany. E-mail: uli.mueller@mx.uni-saarland.de.

DOI:10.1523/JNEUROSCI.0714-14.2014

 0270-6474/14/3416086-07$15.00/0

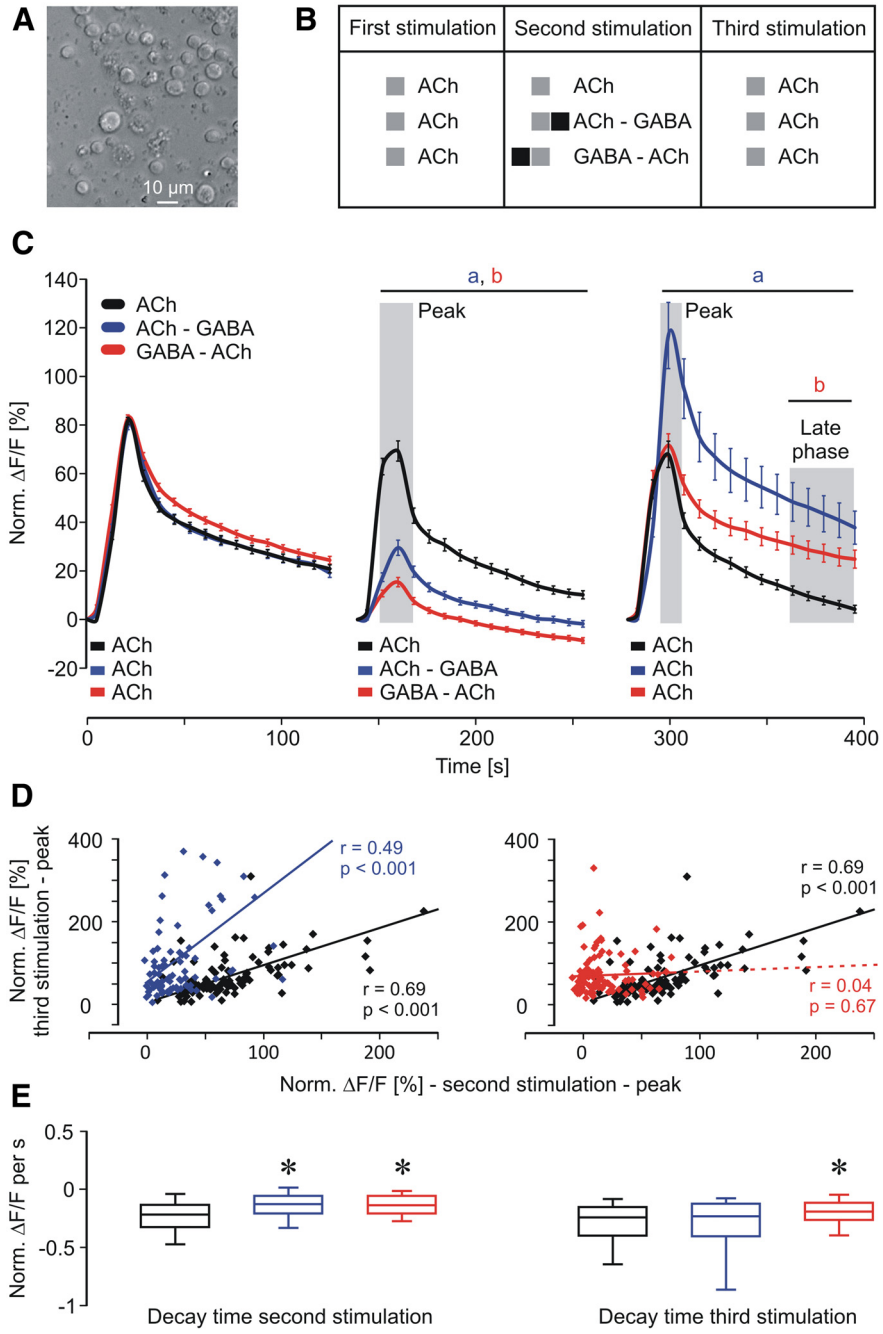

Figure 1. Calcium responses in isolated honeybee KCs during temporal pairing of ACh and GABA. ***A***, Isolated honeybee KCs 24 h after preparation. ***B***, Stimulation scheme. In each experiment isolated KCs received a short pulse of ACh (3 s) as the first stimulus. The second stimulus was ACh (3 s), ACh—GABA, or GABA–ACh (3 s each) followed by the third stimulus, which was ACh (3 s) for all groups. ***C***, Pairing of ACh with GABA significantly inhibited calcium responses during the second stimulation. After ACh–GABA pairing, peak response of the third stimulation was increased while a GABA–ACh pairing led to elevated calcium levels during the late phase (shaded area). Shaded areas around peaks indicate time windows used for correlation analysis in ***D***. The data derived from seven independent measurements (ACh: $n = 110$ neurons; ACh–GABA: $n = 83$ neurons; GABA–ACh: $n = 107$ neurons). Two-way ANOVA followed by Bonferroni *post hoc* test: ***a***, ACh vs ACh–GABA, $p < 0.001$; ***b***, ACh vs GABA–ACh; $p < 0.008$. ***D***, For ACh and ACh–GABA peak responses during second and third stimulation showed strong correlation. No such correlation was observed for GABA–ACh pairing demonstrating substantial pairing-specific differences. Statistics used was the Pearson correlation. ***E***, The decay time in the late phase after ACh–GABA and GABA–ACh pairing is significantly slower compared with ACh alone. During the third stimulation only the GABA–ACh pairing led to a slower decay time, which resulted in elevated calcium levels during the late phase. Kruskal–Wallis one-way ANOVA followed by *post hoc* Dunn's test, $*p < 0.05$.

cholinergic and GABAergic inputs (first ACh, then GABA) critically affects KC signal processing.

To address the question of how the temporal sequence of short GABA and ACh stimuli affects KC activity, we excluded the influence of the neuronal network and visualized calcium activity of isolated KCs. For the whole population of honeybee KCs we demonstrate that distinct features of calcium responses triggered by a paired stimulus depend on the temporal sequence of ACh and GABA. Further we used the genetic tools of *Drosophila* to investigate pairing-specific effects in an exactly defined subset of KCs (201y) implicated in learning in larvae (Pauls et al., 2010) and adults (Zars et al., 2000). In this subset of KCs we also found similar differences as well as a pairing-specific separation of 201y KCs into functional subgroups revealing KCs with different properties and suggesting that these subgroups may contribute to different functions in olfactory processing and learning.

Materials and Methods

Animals

Honeybees. Experiments were conducted year round in Saarbrücken, Germany, using honeybees (*Apis mellifera*) of the University apiary. Foragers were caught in front of hives maintained outdoors in summer or indoors during winter.

Drosophila. Experiments were performed with larvae of a w^+; 201y-GAL4; UAS-Cameleon 2.1 strain, kindly provided by Dr. Andre Fiala (Diegelmann et al., 2002). Flies and larvae were kept at 24°C under a 12 h light/dark regime on modified cornmeal agar medium and yeast (Guo et al., 1996).

Preparation of neurons for imaging

Honeybees. For each experiment the MBs of 8–10 foraging honeybees (females) were dissected and incubated in 200 µl collagenase/dispase mix (1 mg/ml; Sigma-Aldrich) in calcium-free honeybee saline containing the following (in mM): 130 NaCl, 6 KCl, 4 $MgCl_2$, 5 $CaCl_2$, 117 sucrose, 23 glucose, and 10 HEPES, pH 6.7. During 30 min of incubation at 34°C, the tissue was regularly triturated. After the last trituration the tissue settled for 30 s and the supernatant was transferred to a new Eppendorf tube and centrifuged for 3.5 min at 1200 rpm. The new supernatant was discarded and 500 µl of honeybee saline was added. The dissociated cells (10 × 50 µl) were transferred to 10 cover slides coated with poly-L-lysine (0.01%; Sigma-Aldrich) and incubated in a humidity chamber for 1 h to allow the cells to attach to the surface. Before the cells rested overnight the honeybee saline on the coverslips was gently removed and substituted by honeybee medium (L-15 medium; Life Technologies) complemented with the following (in mM): 22 glucose, 14 fructose, 117 sucrose, 29 proline, 13% heat-treated fetal calf serum (PAA), 1% yeastolate (Life Technologies), 1% penicillin-streptomycin mix (10,000 U penicillin, 10 mg/ml streptomycin; Sigma-Aldrich), and 0.1% gentamicin (50 mg/ml; Sigma-Aldrich). Before the measurement cells were incubated for 15 min in 2 µM Fluo-4 AM (Invitrogen). The MB is a well visible structure that can easily be surgically dissected out of the brain. As the MB only contains somata of

KCs, it is assured that the culture only contains KCs, which can be identified by their typical diameters of 7 and 10 μm (Goldberg et al., 1999).

Drosophila. For each experiment the whole brains of 18–21 nonfeeding third-instar larvae (of either sex) were dissected in *Drosophila* saline containing the following (in mM): 130 NaCl, 5 KCl, 2 $MgCl_2$, 2 $CaCl_2$, 36 sucrose, and 5 HEPES, pH 7 (Jan and Jan, 1976). Brains were incubated in 60 μl collagenase/dispase mix (1 mg/ml; Sigma-Aldrich) in calcium-free *Drosophila* saline. After 30 min incubation at 34°C, the tube was centrifuged for 3.5 min at 1600 rpm. The supernatant was discarded and 150 μl medium (TC 100 insect medium; PAA) containing 10% heat-treated fetal calf serum (PAA), 1% penicillin-streptomycin mix (10,000 U penicillin, 10 mg/ml streptomycin; Sigma-Aldrich), and 0.1% gentamicin (50 mg/ml; Sigma-Aldrich) was added. The dissociated cells (3 × 50 μl) were transferred to three coverslips coated with poly-L-lysine (0.01%; Sigma-Aldrich). The coverslips with the cell suspension were incubated in a humidity chamber (25°C) overnight to allow the cells to attach to the surface.

Calcium imaging

A coverslip was mounted into a custom-made flow chamber with a volume of 700 μl. A two-channel pump (Ismatec) provided a constant flow rate of 6 ml/min. After mounting, the neurons were washed with saline for 3–4 min. To mimic temporal aspects of CS–US pairing during associative olfactory conditioning (Raccuglia and Muller, 2013) ACh and GABA were applied subsequently for 3 s. Due to the flow rate and chamber volume ACh and GABA were shortly overlapping, which is an important temporal aspect during conditioning. All drugs (acetylcholine chloride and GABA; both from Sigma-Aldrich), as well as muscimol and 3-APMPA (both from Ascent Scientific), were applied for 3 s by switching between different reservoirs. If not indicated differently, ACh and GABA were used in a concentration of 5 μM for honeybee KCs and 10 μM for *Drosophila* KCs. Muscimol and 3-APMPA were used in a concentration of 10 μM. Picrotoxin (Sigma-Aldrich) was added to the honeybee saline that was constantly perfusing the KCs.

Calcium imaging was performed using an Axiovert 200M microscope (Zeiss) with a Zeiss 20× Plan-Neofluar objective (NA 0.5) and a cooled CCD camera (Cool Snap HQ^2; Photometrics). For Cameleon 2.1 imaging a beam-splitter device with a Cameleon filter set (Dual-View; Optical Insights) was used. Excitation light was provided by a polychrome V system (TILL Photonics) equipped with a computer-controlled shutter. Fluorescent images were collected (1 frame per 1.2 s for Cameleon, *Drosophila* KCs; 1 frame per 1.6 s for Fluo-4 AM, honeybee KCs) at room temperature using SlideBook software. The exposure time per frame was 150 ms for YFP, 300 ms for CFP, and 100 ms for GFP (Fluo-4 AM).

Data processing

Calcium responses were quantified as the percentage change of $\Delta F/F$ for honeybee KCs and $\Delta R/R$ (R = EYFP/ECFP) for *Drosophila* KCs. Baseline fluorescence or baseline ratio was calculated as the average of 5–7 s before stimulation. For all calcium responses each single KC was normalized with respect to the peak induced by the first ACh stimulation, which was defined as 100%. As the temporal kinetics and thus the peak of the individual calcium responses slightly vary, the average peak response is smaller than 100%. Each data point represents the mean (±SEM) of the normalized $\Delta F/F$ or $\Delta R/R$. For temporal smoothing, values of 5 frames each were averaged. KCs that showed no significant ACh-induced peak response during the first stimulation (at least 5% above white noise) were discarded for further statistical evaluation. For correlation between second and third stimulation corresponding values were averaged for each single KC. Decay time for corresponding stimulation was calculated as the derivative of the last 64 s (linear decay). In box plots the ends of the boxes define the 25th and 75th percentiles, and error bars define the 10th and 90th percentiles.

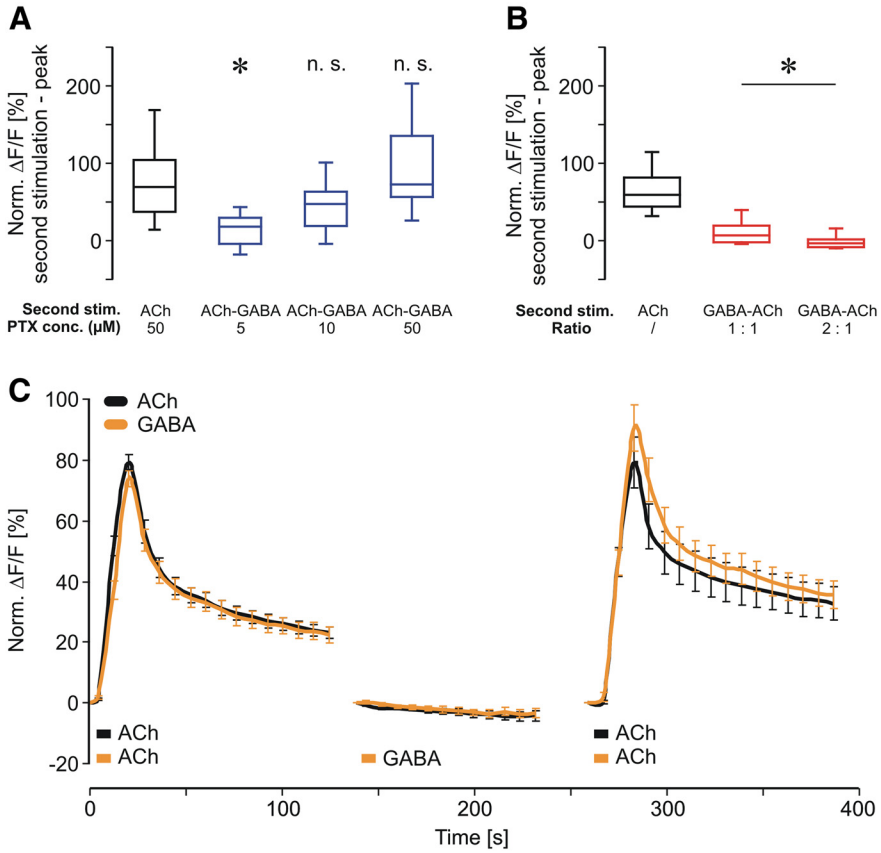

Figure 2. Specificity and concentration dependence of pairing-related inhibition and plasticity. ***A***, Inhibition during ACh–GABA pairing was blocked by the chloride channel blocker PTX. Data derived from two independent measurements for each group (ACh–GABA, 5 μM PTX: $n = 22$; ACh–GABA, 10 μM PTX: $n = 28$; ACh–GABA, 50 μM PTX: $n = 29$; ACh, 50 μM PTX: $n = 36$). Kruskal–Wallis one-way ANOVA followed by *post hoc* Dunn's test, $^*p < 0.05$. ***B***, Elevation of GABA concentration during GABA–ACh pairing increases inhibition. Data derived from at least four independent measurements for each group (ACh: $n = 110$ neurons; GABA–ACh, 1:1: $n = 107$ neurons; GABA–ACh, 2:1: $n = 39$ neurons). Kruskal–Wallis one-way ANOVA followed by *post hoc* Dunn's test, $^*p < 0.05$. ***C***, Presentation of GABA alone has no effect on subsequent third stimulation. Data derived from four independent measurements (ACh: $n = 37$ neurons; GABA: $n = 35$ neurons). Two-way ANOVA followed by Bonferroni *post hoc* test: $p > 0.15$.

Results

We used isolated honeybee KCs to investigate how the temporal contiguity of cholinergic and GABAergic stimuli affects neuronal processing on a cellular level (Fig. 1*A*). To mimic different temporal scenarios of GABA action on ACh-induced calcium signaling we designed a stimulation scheme composed of three groups and three stimulations (Fig. 1*B*). All groups received a first ACh stimulus that served as a reference to normalize the subsequent signals. The second stimulation (after 140 s) either consisted of an ACh–GABA pairing, a GABA–ACh pairing (3 s/3 s), or an ACh stimulation (3 s) alone. After another 140 s, all groups received a third stimulation with ACh to test for effects induced by the previous paired stimulation. A short ACh stimulus led to a fast onset and a slow decay of the calcium response (Fig. 1*C*), which is

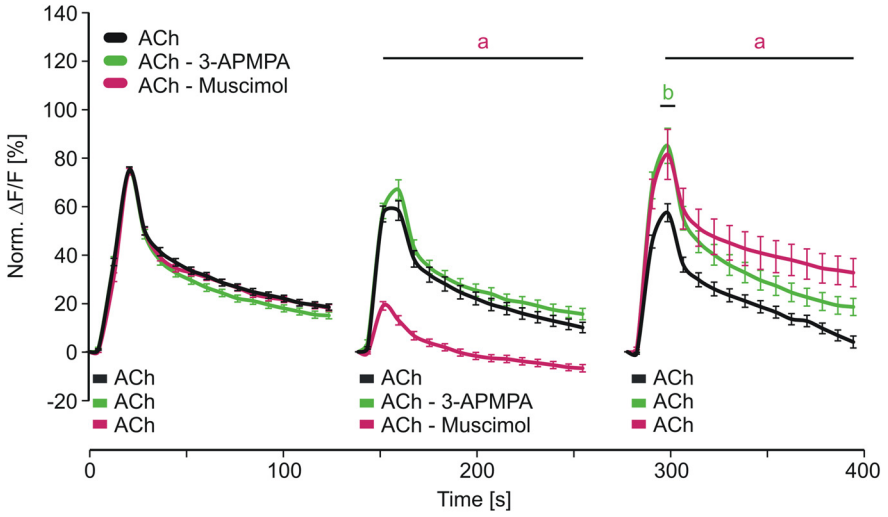

Figure 3. ACh-mediated calcium responses of honeybee KCs are modulated by ionotropic and metabotropic GABA receptors. Inhibition of ACh-induced calcium influx during second stimulation was mediated by ionotropic GABA receptors (selective agonist muscimol). Both, ionotropic and metabotropic (3-APMPA) GABA receptors contributed in facilitating the ACh-induced calcium influx during the third stimulation. Data derived from at least seven independent measurements (ACh: $n = 150$ neurons; ACh–3-APMPA: $n = 141$ neurons; ACh–muscimol: $n = 147$ neurons). Two-way ANOVA followed by Bonferroni *post hoc* test: ***a***, ACh vs ACh–Muscimol; ***b***, ACh vs ACh–3-APMPA; $p < 0.002$.

in accordance with a previous study characterizing the nicotinic ACh receptor-mediated calcium responses in cultured *Drosophila* KCs (Campusano et al., 2007). During the second stimulation the pairing of ACh and GABA led to a significant inhibition of the calcium response [Fig. 1*C*; two-way ANOVA, DF = 2, $F = 877.87$, SEM(ACh) = 0.43, SEM(ACh–GABA) = 0.49, SEM(GABA–ACh) = 0.44, $p < 0.001$; *post hoc* Bonferroni: ACh vs ACh–GABA: $t = 4.57–17.4$, $p < 0.001$, ACh vs GABA–ACh: $t = 7.6–22.09$, $p < 0.001$]. Interestingly, pairing of ACh and GABA led to pairing-specific forms of neuronal plasticity, which affected the processing of the subsequent excitatory stimulus (Fig. 1*C*). The ACh–GABA pairing led to an increase of ACh-induced calcium influx (increased peak response), while the GABA–ACh pairing led to elevated calcium levels during the late phase [two-way ANOVA, DF = 2, $F = 153.92$, SEM(ACh) = 1.16, SEM(ACh–GABA) = 1.34, SEM(GABA–ACh) = 1.18, $p < 0.001$; *post hoc* Bonferroni: ACh vs ACh–GABA: $t = 4.72–7.64$, $p < 0.001$, ACh vs GABA–ACh: $t = 2.88–3.11$, $p < 0.008$]. To investigate the relation between second and third stimulation we analyzed the correlation between peak responses (Fig. 1*D*). For ACh and ACh–GABA pairing, peak responses during second and third stimulation strongly correlated (Fig. 1*D*; Pearson correlation: ACh, $r = 0.69$, $p < 0.001$; ACh—GABA, $r = 0.49$, $p < 0.001$). The distribution of KC responses after the ACh–GABA pairing (third stimulation) displayed a larger range indicating heterogeneity of KC response properties. Interestingly, peak responses during GABA–ACh pairing did not correlate with the peak responses during the third stimulation (Fig. 1*D*; Pearson correlation: GABA—ACh, $r = 0.04$, $p = 0.67$). To test the possibility that the low response levels during the second stimulation induced noise that affected the correlation we eliminated all values <5 and still find no correlation (data not shown; Pearson correlation: GABA—ACh, $r = 0.008$, $p = 0.48$). Therefore the differences in correlation between ACh–GABA and GABA–ACh also indicate pairing-specific effects on the calcium responses of KCs. To investigate how pairing affects calcium kinetics we analyzed the decay time (Fig. 1*E*). During the second stimulation both ACh–GABA and GABA–ACh pairings showed a reduced decay time (Kruskal–Wallis one-way ANOVA, $H = 28$, $p < 0.001$; *post hoc* Dunn's test, ACh vs ACh–GABA: $Q = 4.53$, $p < 0.05$; ACh vs GABA–ACh: $Q = 4.52$, $p < 0.05$). During the third stimulation only GABA–ACh pairing led to a significantly reduced decay time (Kruskal–Wallis one-way ANOVA, $H = 11.6$, $p = 0.003$; *post hoc* Dunn's test, ACh vs ACh–GABA: $Q = 0.33$, $p > 0.05$; ACh vs GABA–ACh: $Q = 3.16$, $p < 0.05$), which explains the elevated calcium levels during the late phase. To specify the GABA receptors involved in mediating inhibition during pairing of ACh and GABA we added the chloride channel blocker picrotoxin (PTX), which completely abolished inhibition during ACh–GABA pairing [Fig. 2*A*; Kruskal–Wallis one-way ANOVA, $H = 38.38$, $p < 0.001$; *post hoc* Dunn's test, ACh vs ACh–GABA (5 μm PTX): $Q = 5.06$, $p < 0.05$; ACh vs ACh–GABA (10 μm PTX): $Q = 2.26$, $p > 0.05$; ACh vs ACh–GABA (50 μm PTX): $Q = 0.99$, $p > 0.05$]. This indicates that inhibition is solely mediated by ionotropic GABA receptors. To investigate how the GABA concentration affects inhibition we compared the calcium responses of equimolar concentrations of GABA and ACh with a twofold increased concentration of GABA (Fig. 2*B*). Increasing the GABA concentration significantly decreased the calcium response during a GABA–ACh pairing, indicating that under equimolar conditions some KCs are not fully inhibited and that the degree of inhibition depends on the properties of single KCs [Kruskal–Wallis one-way ANOVA, $H = 157.93$, $p < 0.001$; *post hoc* Dunn's test, ACh vs GABA–ACh (1:1): $Q = 10.2$, $p < 0.05$; ACh vs GABA–ACh (2:1): $Q = 10.51$, $p < 0.05$, GABA–ACh (2:1) vs GABA–ACh (1:1): $Q = 3.05$, $p < 0.05$]. To test whether GABA alone has any effects on a subsequent excitatory stimulus we applied only GABA during the second stimulation (Fig. 2*C*). The finding that GABA alone neither affected peak response nor decay time of the third stimulation underscores the role of pairing ACh and GABA regarding the pairing-specific neuronal plasticity [two-way ANOVA, DF = 1, $F = 6.64$, SEM(ACh) = 1.33, SEM(GABA) = 1.37, $p = 0.01$; *post hoc* Bonferroni: $t < 1.46$, $p > 0.15$]. To investigate the roles of ionotropic and metabotropic GABA receptors during ACh–GABA pairing we substituted GABA with its specific agonists for ionotropic (muscimol) and metabotropic (3-APMPA) GABA receptors (Fig. 3). 3-APMPA (also SKF97541) has been shown to be a powerful agonist for metabotropic GABA receptors that are formed by the most abundant and highly conserved subunits $GABA_BR1/2$ (Mezler et al., 2001). Inhibition during the second stimulation was only mediated by muscimol confirming that only ionotropic GABA receptors mediate inhibition in KCs [two-way ANOVA, DF = 2, $F = 610.48$, SEM(ACh) = 0.56, SEM(ACh–Muscimol) = 0.56, SEM(ACh–3-APMPA) = 0.58, $p < 0.001$; *post hoc* Bonferroni: ACh vs ACh–muscimol: $t = 5.27–11.92$, $p < 0.001$, ACh vs ACh–3-APMPA: $t < 1.73$, $p > 0.17$]. Interestingly, ionotropic and metabotropic GABA agonists increased ACh-induced calcium influx during the third stimulation, which indicates that both types of GABA receptors contribute in inducing processes of neuronal plasticity [two-way ANOVA, DF = 2, $F = 78.15$, SEM(ACh) = 1.17, SEM(ACh–

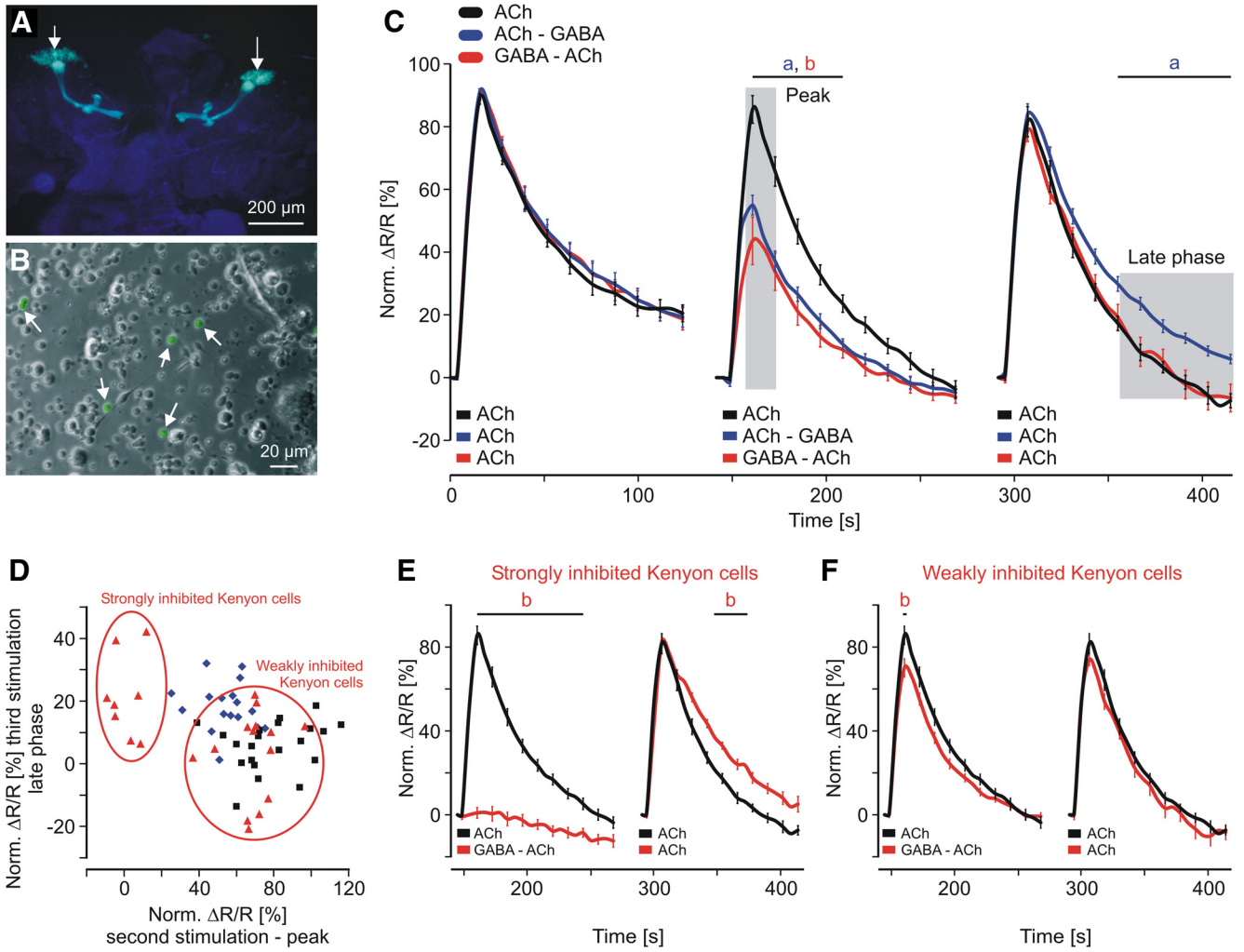

Figure 4. Calcium responses in a defined subset of isolated *Drosophila* KCs during temporal pairing of ACh and GABA. ***A***, Fluorescence image of larval brain whole mount (201y). The calcium-sensitive fluorescence protein cameleon is specifically expressed in a subset of MB KCs involved in learning. ***B***, The isolated KCs were identified by their characteristic cameleon fluorescence (arrows). ***C***, Pairing of ACh and GABA during the second stimulation significantly inhibited the calcium response. ACh–GABA pairing led to elevated calcium levels during the late phase of the third stimulation. Shaded areas indicate averaged time windows used in ***D***. Data derived from at least five independent preparations (ACh: $n = 22$ neurons; ACh–GABA: $n = 17$ neurons; GABA–ACh: $n = 22$ neurons). Two-way ANOVA followed by Bonferroni *post hoc* test: ***a***, ACh vs ACh–GABA; ***b***, ACh vs GABA–ACh; $p < 0.02$. ***D***, Calcium responses for single KCs showed substantial pairing-specific differences and division into subpopulations with different properties. ***E***, ***F***, Strongly inhibited KCs showed no calcium response during the second stimulation and elevated calcium levels during the late phase of the third stimulation. The other subpopulation of KCs was only weakly inhibited and showed no difference during the third stimulation. Two-way ANOVA followed by Bonferroni *post hoc* test: ***b***, ACh vs GABA–ACh; $p < 0.02$.

Muscimol) = 1.18, SEM(ACh–3-APMPA) = 1.2, $p < 0.001$; *post hoc* Bonferroni: ACh vs ACh–Muscimol: $t = 3.24–4.31$, $p < 0.002$, ACh vs ACh-3–APMPA $t = 4.11$, $p < 0.001$].

To study pairing-specific effects in a subpopulation of KCs (201y) that have been shown to be crucial for learning (Zars et al., 2000; Pauls et al., 2010) we used *Drosophila* to express the genetically encoded calcium sensor Cameleon 2.1 (Fig. 4*A*; Diegelmann et al., 2002). The fluorescence of Cameleon, driven by 201y-GAL4 (w^+; 201y-GAL4; UAS-Cameleon 2.1) allowed reliable identification and analysis of defined KCs within a population of dissociated neurons (Fig. 4*B*, white arrows). All KCs that showed an ACh-induced FRET signal significantly above the background signal were included in the analysis (see Materials and Methods). Using this criterion, 94% of the cameleon-labeled KCs responded to a 20 μM ACh stimulus (data not shown; $n = 32$), demonstrating the viability of the measured KCs. To avoid potential saturation effects and to work in the dynamic range, we selected an ACh concentration of 10 μM that activated 41% of the cameleon-labeled KCs (data not shown; $n = 52$). As in the honeybee KCs, we observed inhibition during the second stimulation [two-way ANOVA, DF = 2, $F = 133.51$, SEM(ACh) = 0.7, SEM(ACh–GABA) = 0.8, SEM-(GABA–ACh) = 0.69, $p < 0.001$; *post hoc* Bonferroni: ACh vs ACh–GABA: $t = 2.61–6.3$, $p < 0.02$, ACh vs GABA–ACh: $t = 3.72–9.07$, $p < 0.001$] and pairing-specific forms of neuronal plasticity during the third stimulation (Fig. 4*C*). Different from the honeybee KCs, the *Drosophila* KCs displayed elevated calcium levels of the late phase after the ACh–GABA pairing but no obvious change after the GABA–ACh pairing [two-way ANOVA, DF = 2, $F = 57.87$, SEM(ACh) = 0.68, SEM(ACh–GABA) = 0.77, SEM(GABA–ACh) = 0.67, $p < 0.001$; *post hoc* Bonferroni: ACh vs ACh–GABA: $t = 2.62–3.35$, $p < 0.02$, ACh vs GABA–ACh: $t = 0.05–0.44$, $p = 1$]. To analyze if all KCs display equal degrees of inhibition and calcium levels during the late phase we plotted the corresponding values for each single KC (Fig. 4*D*; due to the low number of neurons, the Pearson correlation was not

performed). Interestingly, GABA–ACh pairing divided the KCs into two subgroups. One subgroup was strongly inhibited by GABA and displayed higher calcium levels during the late phase of the third stimulation (Fig. 4*E*). The other subgroup was only weakly inhibited (Fig. 4*F*) and the third stimulation was not different from the ACh stimulation [two-way ANOVA, second stimulation: DF = 2, $F = 377.7$, SEM(ACh) = 0.7, SEM(GABA–ACh, strongly inhibited) = 0.97, SEM(GABA–ACh, weakly inhibited) = 0.74, $p < 0.001$; *post hoc* Bonferroni: ACh vs GABA–ACh, strongly inhibited: $t = 3.78–15.86$, $p < 0.001$, ACh vs GABA–ACh, weakly inhibited: $t = 3.5$, $p < 0.001$; third stimulation: DF = 2, $F = 52.56$, SEM(ACh) = 0.68, SEM(GABA–ACh, strongly inhibited) = 1.11, SEM(GABA–ACh, weakly inhibited) = 0.85, $p < 0.001$; *post hoc* Bonferroni: ACh vs GABA–ACh, strongly inhibited: $t = 2.6–2.89$, $p < 0.02$, ACh vs GABA–ACh, weakly inhibited: $t < 1$, $p > 0.64$]. These results clearly show that the KCs of the 201y population have different properties that result in different calcium responses within and between the temporal scenarios. As expected, inhibition was modulated depending on the total concentration of the transmitters and the ratio of their concentrations. If GABA was used with a fivefold excess over ACh (10 μM), none of the KCs showed a Ca^{2+} response during the GABA–ACh pairing (data not shown; $n = 32$). Substituting GABA with its specific agonists we found that only muscimol mediates inhibition while 3-APMPA had no effect [data not shown; Kruskal–Wallis one-way ANOVA, $H = 23.5$, $p < 0.001$; *post hoc* Dunn's test, ACh ($n = 12$) vs muscimol–ACh ($n = 15$): $Q = 3.38$, $p < 0.05$; ACh vs 3-APMPA–ACh ($n = 24$): $Q = 0.7$, $p > 0.05$].

Discussion

We demonstrate for the first time that insect KCs are capable of processing cholinergic and GABAergic inputs differently, depending on their temporal sequence. For honeybee KCs, we find that pairing of ACh and GABA inhibits ACh-induced calcium responses. Moreover, we find pairing-specific forms of neuronal plasticity, indicating fundamental differences in the molecular processes induced by the different temporal scenarios. An ACh–GABA pairing (mimics CS–US forward pairing during olfactory conditioning) induces a form of neuronal plasticity that differs from that induced by a GABA–ACh pairing (mimics a US–CS backward-conditioning scenario). The pairing-specific neuronal plasticity overlaps with the time window of successive conditioning trials in honeybee multiple-trial conditioning and short-term memory retrieval in *Drosophila* and thus may play a critical role in processing aspects like repeated conditioning trials, stimulus contiguity, or inhibitory conditioning (Hammer and Menzel, 1995).

Our findings considering the pairing-specific integration of ACh and GABA are also in accordance with the differential temporal role of GABAergic inhibition we observed during olfactory conditioning in honeybees. Focal uncaging of GABA in the mushroom bodies shortly before and during CS–US pairing but not instantly afterward impairs learning (Raccuglia and Mueller, 2013). Thus it is possible that GABA uncaging after CS–US leaves the temporal scenario of a forward-conditioning trial (ACh–GABA) intact, while GABA uncaging before CS–US interferes with the temporal scenario thus impairing learning processes. As in the honeybee KCs we find pairing-specific calcium responses in a subset of *Drosophila* KCs implicated in learning. The inhibitory effect of GABA in the *Drosophila* KCs is smaller than in the honeybee KCs indicating differences in the susceptibility to GABA. Therefore the observed effect on plasticity in *Drosophila* is also smaller, possibly representing differences between two very distinct animals. However, in both organisms the ACh–GABA pairing has a bigger effect on the plasticity of a whole population of KCs, which is in accordance with our theory that this pairing mimics a forward-conditioning scenario, which leads to a more stable form of memory than a backward-conditioning paradigm. Moreover, our data in *Drosophila* suggest that subgroups of KCs contribute differently to processing different temporal scenarios of ACh and GABA. Specifically, the GABA–ACh pairing splits the *Drosophila* KCs into two functional subgroups that greatly differ in their reaction toward GABA. This points to several GABA-mediated modulatory systems in the MB network that could contribute differently to learning. However, future experiments with stringent GAL4 lines combined with elaborate immunohistochemical studies are necessary to test whether specific response properties during pairing are due to individual KC receptor composition. Since our data suggest that the inhibitory action of GABA is mediated by ionotropic GABA receptors, it is very likely that the division into functional subgroups is due to the expression of different subunits that build receptors with very distinct GABA affinity. Of the three subunits identified in *Drosophila*, the well characterized Rdl subunit is critically implicated in olfactory learning (Hosie et al., 1997; Lee et al., 2003; Liu et al., 2007). Alternative splicing and RNA editing of Rdl as well as different subunit compositions provide a "tool box" to generate GABA receptors tuned for very defined functions (GABA EC_{50}s range from ≈3 to 200 μM; Hosie et al., 2001; Jones et al., 2009). A future challenge remains to characterize and manipulate the GABA receptor subunit composition in different populations of KCs, to understand their contribution to associative learning in *Drosophila*. The conservation of $GABA_A$ receptors makes it likely that the differential computations determined by the temporal sequence of excitatory and inhibitory inputs may be an evolutionary conserved feature that applies to inhibitory networks of all species.

References

Campusano JM, Su H, Jiang SA, Sicaeros B, O'Dowd DK (2007) nAChR-mediated calcium responses and plasticity in *Drosophila* Kenyon cells. Dev Neurobiol 67:1520–1532. CrossRef Medline

Collinson N, Kuenzi FM, Jarolimek W, Maubach KA, Cothliff R, Sur C, Smith A, Otu FM, Howell O, Atack JR, McKernan RM, Seabrook GR, Dawson GR, Whiting PJ, Rosahl TW (2002) Enhanced learning and memory and altered GABAergic synaptic transmission in mice lacking the alpha 5 subunit of the GABAA receptor. J Neurosci 22:5572–5580. Medline

de Belle JS, Heisenberg M (1994) Associative odor learning in *Drosophila* abolished by chemical ablation of mushroom bodies. Science 263:692–695. CrossRef Medline

DeLorey TM, Handforth A, Anagnostaras SG, Homanics GE, Minassian BA, Asatourian A, Fanselow MS, Delgado-Escueta A, Ellison GD, Olsen RW (1998) Mice lacking the beta3 subunit of the GABAA receptor have the epilepsy phenotype and many of the behavioral characteristics of Angelman syndrome. J Neurosci 18:8505–8514. Medline

Diegelmann S, Fiala A, Leibold C, Spall T, Buchner E (2002) Transgenic flies expressing the fluorescence calcium sensor Cameleon 2.1 under UAS control. Genesis 34:95–98. CrossRef Medline

Goldberg F, Grünewald B, Rosenboom H, Menzel R (1999) Nicotinic acetylcholine currents of cultured Kenyon cells from the mushroom bodies of the honey bee Apis mellifera. J Physiol 514:759–768. CrossRef Medline

Gronenberg W (1987) Anatomical and physiological properties of feedback neurons of the mushroom bodies in the bee brain. Exp Biol 46:115–125. Medline

Grünewald B (1999) Morphology of feedback neurons in the mushroom body of the honeybee, *Apis mellifera*. J Comp Neurol 404:114–126. CrossRef Medline

Guo A, Li L, Xia SZ, Feng CH, Wolf R, Heisenberg M (1996) Conditioned visual flight orientation in *Drosophila*: dependence on age, practice, and diet. Learn Mem 3:49–59. CrossRef Medline

Hammer M, Menzel R (1995) Learning and memory in the honeybee. J Neurosci 15:1617–1630. Medline

Hosie AM, Aronstein K, Sattelle DB, ffrench-Constant RH (1997) Molecular biology of insect neuronal GABA receptors. Trends Neurosci 20:578–583. CrossRef Medline

Hosie AM, Buckingham SD, Presnail JK, Sattelle DB (2001) Alternative splicing of a *Drosophila* GABA receptor subunit gene identifies determinants of agonist potency. Neuroscience 102:709–714. CrossRef Medline

Jan LY, Jan YN (1976) Properties of the larval neuromuscular junction in *Drosophila melanogaster*. J Physiol 262:189–214. Medline

Jones AK, Buckingham SD, Papadaki M, Yokota M, Sattelle BM, Matsuda K, Sattelle DB (2009) Splice-variant- and stage-specific RNA editing of the *Drosophila* GABA receptor modulates agonist potency. J Neurosci 29:4287–4292. CrossRef Medline

Lee D, Su H, O'Dowd DK (2003) GABA receptors containing Rdl subunits mediate fast inhibitory synaptic transmission in *Drosophila* neurons. J Neurosci 23:4625–4634. Medline

Lin AC, Bygrave AM, de Calignon A, Lee T, Miesenböck G (2014) Sparse, decorrelated odor coding in the mushroom body enhances learned odor discrimination. Nat Neurosci 17:559–568. CrossRef Medline

Liu X, Davis RL (2009) The GABAergic anterior paired lateral neuron suppresses and is suppressed by olfactory learning. Nat Neurosci 12:53–59. CrossRef Medline

Liu X, Krause WC, Davis RL (2007) GABAA receptor RDL inhibits *Drosophila* olfactory associative learning. Neuron 56:1090–1102. CrossRef Medline

Mezler M, Müller T, Raming K (2001) Cloning and functional expression of GABA(B) receptors from *Drosophila*. Eur J Neurosci 13:477–486. CrossRef Medline

Pauls D, Selcho M, Gendre N, Stocker RF, Thum AS (2010) *Drosophila* larvae establish appetitive olfactory memories via mushroom body neurons of embryonic origin. J Neurosci 30:10655–10666. CrossRef Medline

Pitman JL, Huetteroth W, Burke CJ, Krashes MJ, Lai SL, Lee T, Waddell S (2011) A pair of inhibitory neurons are required to sustain labile memory in the *Drosophila* mushroom body. Curr Biol 21:855–861. CrossRef Medline

Raccuglia D, Mueller U (2013) Focal uncaging of GABA reveals a temporally defined role for GABAergic inhibition during appetitive associative olfactory conditioning in honeybees. Learn Mem 20:410–416. CrossRef Medline

Vogels TP, Sprekeler H, Zenke F, Clopath C, Gerstner W (2011) Inhibitory plasticity balances excitation and inhibition in sensory pathways and memory networks. Science 334:1569–1573. CrossRef Medline

Zars T, Fischer M, Schulz R, Heisenberg M (2000) Localization of a short-term memory in *Drosophila*. Science 288:672–675. CrossRef Medline